Fast extremum seeking using multisine dither and online complex curve fitting

Thijs van Keulen [*,**] **Robert van der Weijst** [*] **Tom Oomen** [*]

[*] *Eindhoven University of Technology, Dept. of Mech. Engineering, Control Systems Technology group, Eindhoven, the Netherlands (e-mail: t.a.c.v.keulen(at)tue.nl)*
[**] *ASML, Veldhoven, the Netherlands*

Abstract: Fast online optimization of uncertain Wiener systems using extremum seeking control (ESC) is investigated. Derivative estimation in extremum seeking is herefore described as an online parametric system identification problem. Multisine dithering is applied with frequencies around the first resonance frequency of the system to remove the time scale separation between dither and plant dynamics which is commonly required in ESC. Recursive use of the Fourier transform, over a moving window of historic data, provides a frequency response function estimate of the system's local best linear approximation. Continuous online complex curve fitting is then applied to extrapolate to an estimate of the steady-state response which coincides with the local gradient of the steady-state objective function. An analysis of the closed-loop dynamics is provided. Transient improvements and robustness of the approach against plant variation are demonstrated with a simulation example.

Keywords: Extremum seeking and model-free adaptive control, closed-loop identification, frequency domain identification

1. INTRODUCTION

It lies at the heart of human engineering to operate systems in an optimal way. For instance, it can be an objective to minimize energy consumption, to optimize a process output, or to maximize the throughput of a system. One way to achieve optimality is to use detailed modeling such that optimal control settings can be predicted (Skogestad, 2000). However, these model-based approaches lack robustness in achieving optimality, either because the cost of the system is too complex to be modeled accurately, or the system suffers from unknown disturbances, e.g., due to slow transients, changing environmental conditions, production tolerances, fouling or wear.

Extremum Seeking Control (ESC) is a data-driven control approach for online optimization of systems and processes that adds robustness to the optimization process. Under the assumption that a cost can be measured online, and there is a convex-like relation, in steady-state, between the input of the system and the cost, a feedback loop can be designed that adapts the system input such that the derivative of the cost with respect to the input is directed to a derivative of value zero which results in (local) optimization of the steady-state cost.

Classical ESC provides optimization of the steady-state cost of an unknown plant. This is achieved by injection of a sinusoidal dither signal to estimate the local derivative of the steady-state cost function and to adjust the control input by a steepest descent feedback control. Classical ESC convergence results (Krstic and Wang, 2001; Nesic et al., 2010) hinge on time scale separation between the fast system dynamics and the slow dither frequency. This time scale separation, however, limits the adaptation speed.

A key objective in ESC is fast convergence to the optimum. Convergence speed can be enhanced if prior knowledge of the system dynamics is exploited. In Krstic (2000) and Haring et al. (2013), faster convergence is achieved with phase compensation which allows to perturb the system with a higher frequency under the assumption that the system's phase lag at the dither frequency is known.

Similarly, the design of the ESC scheme in Moase and Manzie (2012) and Atta and Guay (2017) exploits knowledge of the relative order of the linear dynamics of a Hammerstein plant. The technique uses compensation of the high-frequency phase-shift associated with the system's relative order. Hence, these approaches allow for the use of high perturbation frequencies relative to the plant dynamics.

The fast ESC approaches demonstrate significant improvements in transient performance. However, the existing approaches for fast ESC strongly depend on prior knowledge of the system dynamics at high frequencies, and are, therefore, sensitive to system uncertainty. Also, at frequencies beyond the system dynamics, the frequency response gain is typically low which might lead to sensing and actuation limitations in the presence of measurement noise.

Although important progress is made to improve convergence speed of ESC algorithms, at present these approaches strongly depend on prior knowledge. The aim of this paper is to develop an approach for fast ESC for Single-Input-Single-Output (SISO) systems which does not require accurate system knowledge. In sharp contrast,

the key idea is to locally estimate the system, which is in line with recent developments in nonparametric identification of frequency response functions using local parametric models, see Van Keulen et.al. (2017).

The method applies a multisine dither signal with frequencies in the same time scale as the system dynamics, e.g., around the first resonance frequency of the system. Past data of the input and cost output is stored in a moving time window with a length equal to the multisine time period. Using the Fourier Transform (FT), the Best Linear Approximation (BLA) of the underlying transfer function of the local linear system can be estimated at the multisine dither frequencies (Pintelon and Schoukens, 2001). Next, online complex curve fitting (Van Herpen et al., 2014; Levy, 1959; Sanathanan and Koerner, 1963; Voorhoeve et al., 2014) is applied to estimate the steady-state gain of the response which relates to the local gradient of the steady-state performance function. As long as the optimizer time scale is slow compared to the dither frequencies, the BLA estimate is accurate.

The main contribution of this paper is to achieve fast Derivative Estimator (DE) in an ESC framework with robustness to system uncertainty. The key difference compared to earlier approaches is to allow for high-frequency perturbation of the system without the requirement to know the exact system's order or phase lag at a particular frequency.

This article is structured as follows. In Section 2, a problem description is provided. Section 3 gives an overview of the approach. An analysis of the closed-loop behavior is provided in Section 4. In Section 5, the theory is supported with a simulation example. Finally, in Section 6, conclusions and outlook on future research are provided.

2. PROBLEM DESCRIPTION AND ASSUMPTIONS

Consider the optimization of the following SISO Wiener system with a linear dynamic object and a static nonlinear output characteristic:

$$\dot{x}(t) = Ax(t) + Bu(t), \tag{1}$$
$$y(t) = h(x(t)), \tag{2}$$

where $u \in \mathbb{R}$ is the control input, $x \in \mathbb{R}^l$ the state vector, $A \in \mathbb{R}^{l\times l}$ the constant state matrix, $B \in \mathbb{R}^{l\times 1}$ the input matrix and, $h \in \mathbb{R}$ a nonlinear output function.

Loosely speaking, the ESC objective is to steer the input u to a value that optimizes the steady-state cost y. Assumptions are imposed to ensure convergence of the ESC loop. The following assumption states that the system exhibits stability properties and possesses a steady-state performance map.

Assumption 1 *For any constant input u, the system possesses a unique, asymptotically stable equilibrium $x_{eq} = -A^{-1}Bu$, i.e. where $Ax + Bu = 0$, such that the cost output y is described by the steady-state performance map $Q_y : u \to y$ given by:*

$$Q_y(u) = h(-A^{-1}Bu). \tag{3}$$

Linearization of the dynamic system (1) to (2), at the equilibrium x_{eq}, and subsequent application of the Laplace transform, provides the following transfer function:

$$H(s,u) = \tilde{C}(u)\,(sI - A)^{-1}\,B, \tag{4}$$

where $\tilde{C}(u) := \left.\frac{\mathrm{d}y(x)}{\mathrm{d}x}\right|_{x_{eq}}$. Note that, $\tilde{C}(u)$ is a frequency independent scaling factor while the denominator of H is time invariant and independent of the equilibrium.

Lemma 1 *Given* (1) *and* (2)*, and let Assumption 1 hold, then the DE of the steady-state performance map at u coincides with the steady-state gain of the transfer function of the system linearized at u:*

$$\frac{dQ_y(u)}{du} = H(0,u). \tag{5}$$

Proof Evaluating (4) at $s = 0$ provides $H(0,u) = -\tilde{C}(u)A^{-1}B$. Derivation of (3) with respect to u gives $\frac{dQ_y}{du} = \frac{dh(-A^{-1}Bu)}{dx}\frac{dx}{du}$. By using $\tilde{C}(u) := \left.\frac{\mathrm{d}y(x)}{\mathrm{d}x}\right|_{x_{eq}}$ and $\frac{x_{eq}}{u} = -A^{-1}B$, it follows that $\frac{dQ_y(u)}{du} = H(0,u)$. □

In addition to Assumption 1, the following assumption is imposed, which ensures the existence of a unique extremum and monotonic convergence towards that extremum of the map $Q_y(u)$.

Assumption 2 *The mapping $Q_y(.)$ is 2 times continuously differentiable and there exists a constant input u^* such that the gradient*

$$g(u) := \frac{dQ_y(u)}{du} = 0, \tag{6}$$

if and only if $u = u^*$, and

$$\frac{d^2Q_y(u)}{du^2} > 0. \tag{7}$$

Observe that, using Assumption 1 and 2, and Lemma 1, it follows that $H(0,u) = 0$ if and only if $u = u^*$.

The objective of the ESC is to adjust u such that the steady-state performance map $Q_y(u)$ is minimized, i.e. to find the unknown optimizing input:

$$u^* = \arg\min_u(Q_y(u)). \tag{8}$$

Assumptions 1 and 2 are common in classical ESC, see again Krstic and Wang (2001); Nesic et al. (2010). To enable the fast ESC approach outlined in this paper, the following assumption is added:

Assumption 3 *The system can locally be approximated by a low-order continuous-time rational-form parametric model approximation:*

$$H_a(s) = \frac{Q(s)}{P(s)} = \frac{\sum_{r=0}^{n_q} q_r s^r}{\sum_{r=0}^{n_p} p_r s^r}, \tag{9}$$

of system (4) *for which* $\sup_{\omega\in[0\ \omega_q]} |H(j\omega) - H_a(j\omega)| \le \epsilon_H$*. Where $\epsilon_H > 0$ is a positive constant, ω_q is the frequency up to which accurate model information is available, and $q_r, p_r \in \mathbb{R}$.*

Assumption 3 enables that the system's fast dynamics, i.e. above ω_q, can be ignored. However, it is assumed that a low-order approximate of the system is available.

Remark 1 *A suitable low-order approximation for the system dynamics can be obtained with offline system identification at some constant u. Explicit knowledge of* (2) *is*

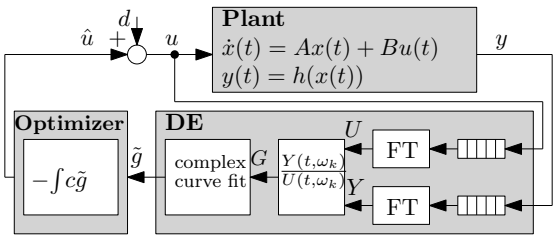

Fig. 1. Schematic overview of the fast ESC loop.

not required, i.e. the ESC scheme provides robustness to the optimization process.

3. FAST EXTREMUM SEEKING USING MULTISINE EXCITATION AND ONLINE COMPLEX CURVE FITTING

3.1 Overview of the approach

Figure 1 provides a schematic of the envisioned fast ESC approach. Similar to classical ESC, the loop contains a DE and an optimizer. Essentially, the ESC follows a continuous steepest-descent optimization approach where locally a gradient of Q_y in u is estimated and the function value is optimized by integration of the DE. However, this DE is more involved than the classical implementation.

Frequency-based evaluation is recursively applied to past data of input u and output y stored over a finite interval with length T in a moving horizon fashion. Next, the FT of both the input and output signal is derived and the Frequency Response Function (FRF) is computed. A parametric plant model is estimated on the FRF using complex curve fitting.

A DE of the steady-state performance map is then obtained by evaluating the steady-state response of the fitted local linear continuous-time dynamic model. Finally, an integral-type optimizer is applied to steer the plant input towards the optimizing value u^* in (8).

3.2 Multisine dither signal

The multisine dither signal is defined as:

$$d(t) = \sum_{k=0}^{N_k} a \cos\left(\omega_k t + \phi_k\right), \tag{10}$$

in which $N_k + 1$ is the number of harmonics present in the multisine, a the amplitude which for simplicity is kept constant for all dither frequencies, and, ω_k and ϕ_k are the respective, frequency and phase of the k-th sinusoid. A random phase multisine is considered since it results in a small peak variation of d.

The dither signal is added to the input of the plant:

$$u(t) = \hat{u}(t) + d(t), \tag{11}$$

where $\hat{u}(t)$ is the optimizer output.

3.3 Online frequency response function measurements

The window time T over which the online FT is computed is chosen to be $T = 2\pi/\omega_0$ and the higher dither frequencies are restricted to be integer multiples of ω_0 such that the dither signal has an integer number of periods of each sinusoid in the window.

The FT, at time instance t, of the input and output signal, is given by:

$$U(t,k) = \frac{1}{T}\int_{t-T}^{t} u(\sigma) e^{-jkt\omega_0} \mathrm{d}\sigma, \tag{12}$$

$$Y(t,k) = \frac{1}{T}\int_{t-T}^{t} y(\sigma) e^{-jkt\omega_0} \mathrm{d}\sigma, \tag{13}$$

in which, $U(t,k)$ and $Y(t,k)$ are the response at the k^{th} dither frequency, of the input and output, respectively.

Application of the FT to the measured input and output signals provides a measurement of the FRF and an estimate of the underlying transfer function at N_k frequencies:

$$G(t,\omega_k) = Y(t,k)/U(t,k), \tag{14}$$

where $G(t,\omega_k)$ is the measured FRF of the plant at the corresponding k dither frequencies, at time instance t in the receding horizon.

3.4 Complex curve fitting

The FRF (14) provides information of the system's local dynamics at the dither frequencies. However, the ESC objective is to improve the steady-state cost (3) which requires a DE of the system's steady-state performance map. So, the estimation of the steady-state response requires an extrapolation from high-frequency response function information at the dither frequencies to the steady-state response. To extrapolate, a parametric model fit is used.

Therefore, consider a continuous-time rational-form parametric model of the form:

$$\tilde{H}(s,\theta(t)) = \theta(t) H_a(s). \tag{15}$$

Here, $\tilde{H} \in \mathcal{H}(s)$ is the parametric model fit obtained within the model set $\mathcal{H}(s)$ according to Assumption 3, and θ is the unknown model parameter at time instance t. Given Assumption 1, it follows that the system is stable and has no poles on the imaginary axis which makes the steady-state response finite and constant.

The plant model parameter θ is obtained by minimizing the sum of squared residuals:

$$V(\theta(t)) := \sum_{k=0}^{N_k} \left| W(\omega_k)\left(G(t,\omega_k) - \tilde{H}(\omega_k,\theta(t))\right)\right|^2, \tag{16}$$

where, $W(\omega_k)$ is a frequency-dependent weighting function, and $G(t,\omega_k)$ is given by the FRF in (14). In Levy (1959), the solution $\theta(t)$ is obtained by minimization of (16).

It is known (Sanathanan and Koerner, 1963; Voorhoeve et al., 2014), that (16) can overemphasis high-frequency errors. Therefore, it is suggested to adapt the weighting of the cost function (16) with $W(\omega_k) = \frac{1}{|Q(j\omega)|^2}$. Where Q is the nominator of H_a in (9).

Frequency responses W, G and H_a have real and imaginary components:

$$W(j\omega_k)G(t,j\omega_k) = \alpha(t,\omega_k) + j\beta(t,\omega_k), \tag{17}$$

$$W(j\omega_k)H_a(j\omega_k) = \gamma(\omega_k) + j\kappa(\omega_k). \tag{18}$$

Moreover, V is quadratic in θ. Hence, the value $\theta \in \mathbb{R}$ that minimizes V, satisfies $\frac{\partial V(\theta)}{\partial \theta} = 0$, therefore:

$$\theta(t) = \frac{1}{N_k + 1} \sum_{k=0}^{N_k} \frac{\alpha(t, \omega_k)\gamma(\omega_k) + \beta(t, \omega_k)\kappa(\omega_k)}{\gamma^2(\omega_k) + \kappa^2(\omega_k)}. \quad (19)$$

Using Lemma 1, an estimate of the local gradient of the steady-state performance map Q_y can be derived from the fitted dynamic plant model evaluated at $\omega = 0$:

$$\tilde{g}(t) := \tilde{H}(0, \theta(t)) = \theta(t)\frac{q_0}{p_0}. \quad (20)$$

Remark 2 *It is possible to extend the complex curve fitting to multiple model parameters. Hereby reducing the need for an accurate model H_a. However, it is shown in Whitfield (1989) that, the fixed point to which subsequent SK-iterations are converging, generally, does not correspond to a (local) minimum of criterion* (16)*. Nevertheless, it is possible to replace the adaptive updating of weighting W after a few iterations by Gauss-Newton iterations which guarantee convergence to a (local) minimum, see (Pintelon and Schoukens, 2001, Section 7.9.1). Also, in Van Herpen et al. (2014), an optimally conditioned Instrumental Variable approach is formulated as an alternative frequency domain identification algorithm, potentially enabling global convergence with an increase of algorithm efficiency.*

3.5 Optimizer

Online optimization of the steady-state cost is achieved by adjusting $\hat{u}$ by a steepest-descent optimization algorithm:

$$\dot{\hat{u}}(t) = -c\tilde{g}(t), \quad (21)$$

where $\tilde{g}$ is the DE by (20) and $c > 0$.

4. ANALYSIS OF CLOSED-LOOP DYNAMICS

The main contribution of fast ESC is convergence analysis without restrictive requirements on time scale separation between the dither signal and plant dynamics. However, the usual assumption that c in (21) is sufficiently small is adopted such that the ESC loop is slow compared to the dither frequencies and plant dynamics.

The objective of this section is to demonstrate the removal of time scale separation between dither and plant dynamics. To this end, the following steps are considered: 1) accuracy of the FT in the presence of nonlinear distortions, 2) accuracy of the complex curve fit, 3) description of the plant and DE time scales, 4) description of the closed-loop dynamics.

4.1 Accuracy of the Fourier transform

The accuracy of the FT relies on recursive identification of a linear dynamic system in the presence of a nonlinear distortion. The measured FRF in (14) consists of

$$G(j\omega_k) = G_{BLA}(j\omega_k) + G_s(j\omega_k), \quad (22)$$

where G_{BLA} is the BLA to the nonlinear system and G_s is a stochastic nonlinear contribution. To the complex curve fitting of Section 3.4 G_s will look like noise, and the effects are smoothed out, see Crama and Schoukens (2005).

The BLA has two contributions:

$$G_{BLA}(j\omega_k) = G_0(j\omega_k) + G_B(j\omega_k). \quad (23)$$

Here, G_0 is the local linear approximation of the underlying dynamic system and G_B a systematic error due to nonlinearity (Pintelon and Schoukens, 2001).

For Wiener system (1) to (2), excited with a random phase multisine, it follows that (Pintelon and Schoukens, 2001, Section 3.4.3.5):

$$G_{BLA}(j\omega_k) = K(a, H)H(j\omega_k). \quad (24)$$

The asymptotic BLA G_{BLA} equals the linear system within a real frequency-independent scale factor K. For sufficiently small amplitudes a the linear contribution dominates the nonlinear one, hence, $G(j\omega_k) \approx H(j\omega_k)$.

4.2 Accuracy of the complex curve fit

Criterion V is quadratic in parameter θ. Hence, (19) provides the global minimum. So, given that the FRF measurement $G(j\omega_k)$ at the dither frequencies is accurate, it follows from Assumption 3 that the gradient estimation error is bounded $|H(0) - \theta H_a(0)| < \epsilon_H$.

4.3 Time scale analysis

Let (A_p, B_p, C_p) be a minimal realization of stable system (4) in Jordan canonical form with state-space equations:

$$\frac{dx(t)}{dt} = A_p x(t) + B_p u(t), \quad (25)$$

$$y(t) = C_p x(t), \quad (26)$$

in which $A_p = \begin{bmatrix} \omega_{p_1} & & \\ & \omega_{p_2} & * \\ & 0 & \ddots \\ & & \omega_{p_m} \end{bmatrix}$. Here, eigenvalues ω_{p_i} are ordered $|\omega_{p_1}| \leq |\omega_{p_2}| \leq \ldots \leq |\omega_{p_m}|$. The time scale of the system (1)-(2) can be characterized by the eigenfrequency ω_{p_1} of the slowest pole.

Suppose now that, Assumption 3 holds for high enough frequency $\omega_q > \omega_{N_k}$ such that the slowest dither frequency $\frac{\omega_0}{\pi} \approx \omega_{p_1}$, i.e. the multisine dither lies in the time scale of the plant dynamics, then A_p in (25) can be scaled such that:

$$\frac{dx(t)}{dt} = \frac{\omega_0}{\pi}\tilde{A}_p x(t) + B_p u(t), \quad (27)$$

where the first entry of $\tilde{A}_p$ is $\frac{\pi\omega_{p_1}}{\omega_0} \approx 1$.

4.4 Time scale of the estimated derivative

The FT described by (12) to (13) is a Moving-Average Filter (MAF) with a time scale of $T = 2\pi/\omega_0$. Observe that, calculations (14), (19) and (20) are algebraic and do not lead to additional delay in the DE. The MAF works as an ideal low-pass filter for input frequency components that are periodic in T, see Robles et al. (2010).

The MAF transfer function for (12) and (13) is given by:

$$\Psi(s, k) = \frac{1 - e^{-Ts}}{Ts} \approx \frac{\omega_0}{\pi s + \omega_0}, \quad (28)$$

where the approximate is based on a first order Pade approximation of the delay term $e^{-Ts} \approx \frac{1 - Ts/2}{1 + Ts/2}$.

Furthermore, assuming that the change in u and y is small compared to the dither induced oscillation, the approximate of the delayed and averaged frequency content, at the N_k dither frequencies, of (12) and (13) is given by:

$$\dot{U}^a(t,a,k) \approx -\tfrac{\omega_0}{\pi}[U^a(t,a,k) + \mu_u(a,u^a,k)u^a(t)], \quad (29)$$

$$\dot{Y}^a(t,a,k) \approx -\tfrac{\omega_0}{\pi}[Y^a(t,a,k) + \mu_y(a,u^a,k)y^a(t)], \quad (30)$$

Here, u^a is the averaged input and $y^a = h(-\tilde{A}_p^{-1}Bu^a)$, μ_u and μ_y relate to the computation of the signal frequency content of u and y, respectively.

4.5 Description of the closed-loop dynamics

The aim of the framework is to demonstrate stability of the closed-loop system by combining the continuous optimization (21) with the plant dynamics and DE in a way that the closed-loop dynamics approximates the behavior of (21) which is in line with Nesic et al. (2010).

Introduce $\tilde{u} = \hat{u} - u^*$ and $\tau = \frac{\omega_0}{\pi}\delta t$ in new time scale τ. Here, $\delta \in \mathbb{R}$ is a tuning variable $0 < \delta \ll 1$. The closed-loop dynamics of the system in Fig. 1 are given, in standard singular perturbation form, by:

$$\frac{d\tilde{u}^a(\tau)}{d\tau} = f(a,\epsilon_H,U^a,Y^a), \quad (31)$$

$$\delta\frac{dU^a(\tau)}{d\tau} = -U^a(\tau,a,k) + \mu_u(a,u^a,k)u^a(\tau), \quad (32)$$

$$\delta\frac{dY^a(\tau)}{d\tau} = -Y^a(\tau,a,k) + \mu_y(a,u^a,k)y^a(\tau), \quad (33)$$

$$\delta\frac{dx^a(\tau)}{d\tau} = \tilde{A}_p x^a(\tau) + B_p u^a(\tau). \quad (34)$$

Here, parameter c in (21) is replaced by $\frac{\omega_0}{\pi}\delta$ and $f(.)$ is a static nonlinear mapping defined by (14), (19) and (20). This demonstrates that the DE operates in the same time scale as the system dynamics.

Next, "freeze" U^a, Y^a and x^a, at their equilibria $U^a = \mu_u(a,u^a,k)u^a$, $Y^a = \mu_y(a,u^a,k)y^a$ and $x^a = -\tilde{A}^{-1}Bu^a$, i.e. as $\delta \to 0$, to obtain the reduced system in u^r:

$$\frac{du^r}{d\tau} = -f(a,\epsilon_H,U^a,Y^a). \quad (35)$$

Finally, convergence of the ESC loop is demonstrated with application of Nesic et al. (2010, Theorem 1). Let $z_u(t) = U^a - \mu_u(a,u^a,k)u^a$, $z_y(t) = Y^a - \mu_y(a,u^a,k)y^a$, $z_x(t) = x^a + \tilde{A}^{-1}Bu^a$, and $z = [z_u\ z_y\ z_x]$.

Assumption 4 A function $\beta : \mathbb{R}_{\geq 0} \times \mathbb{R}_{\geq 0} \to \mathbb{R}_{\geq 0}$ is of class $\mathcal{KL}$ if it is strictly increasing in the first argument and strictly decreasing to zero in its second argument. There exists $\beta_u \in \mathcal{KL}$ such that the following holds: for any positive pair (Δ,ν), there exists $\epsilon^* > 0$ such that for any $\epsilon \in (0,\epsilon^*)$ and $||w||_\infty \leq \epsilon$ the solutions of the system $\dot{u} = -f(a,\epsilon,U^a,Y^a) + w(t)$ satisfy $|u(t) - u^*| \leq \beta_u(|u(0) - u^*|,t) + \nu$, for all $|u(0) - u^*| \leq \Delta$.

Theorem 1: Suppose that Assumptions 1, 2 and 4 holds. Then, there exists β_u and $\beta_z \in \mathcal{KL}$ such that the following holds: for any given positive pair (Δ,ν), there exists $\omega_0^* > 0$ and $a^* > 0$ such that for any $\omega_0 \in (0,\omega_0^*)$ and any $a \in (0,a^*)$, there exists $\delta^*(a) > 0$ such that for any $\delta \in (0,\delta^*(a))$, the solutions of the system satisfy

$$|\tilde{u}(t)| \leq \beta_u\left(|\tilde{u}(t_0)|, \tfrac{\omega_0}{\pi}\delta(t-t_0)\right) + \nu, \quad (36)$$

$$|z(t)| \leq \beta_z\left(|z(t_0)|, \tfrac{\omega_0}{\pi}(t-t_0)|\right) + \nu, \quad (37)$$

for all $|[\tilde{u}(t_0)\ z(t_0)]^\top| \leq \Delta$ and $t \geq t_0 \geq 0$.
Proof: see Appendix in Nesic et al. (2010).

The application of Nesic et al. (2010, Theorem 1) demonstrates that the output of the system can be regulated arbitrarily close to the extremum value $Q_y(u^*)$ by adjusting tuning variables a, δ and ϵ_H.

5. EXAMPLE

To illustrate the performance gain of fast ESC over classical ESC, the following Wiener system with six'th order dynamics is used:

$$\dot{x}_1(t) = x_2(t) - u(t), \quad (38)$$

$$\dot{x}_2(t) = -\omega_{p_1}^2 x_1(t) - 2\beta_1\omega_{p_1}x_2(t), \quad (39)$$

$$\dot{x}_3(t) = x_4(t) - x_2(t), \quad (40)$$

$$\dot{x}_4(t) = -\omega_{p_2}^2 x_3(t) - 2\beta_2\omega_{p_2}x_4(t), \quad (41)$$

$$\dot{x}_5(t) = x_6(t) - x_4(t), \quad (42)$$

$$\dot{x}_6(t) = -\omega_{p_3}^2 x_5(t) - 2\beta_3\omega_{p_3}x_6(t), \quad (43)$$

$$y(t) = x_6^2(t), \quad (44)$$

in which, $u(t)$ is the input variable, $y(t)$ the cost output variable, x_1-x_6 the state variables, $\omega_{p_1} = 2\pi$, $\omega_{p_2} = 10\pi$, $\omega_{p_3} = 14\pi$ are the resonance frequencies, and $\beta_1 = 0.2$, $\beta_2 = 0.025$, $\beta_3 = 0.025$ are the dampling factors. The steady-state cost function is given by:

$$Q_y(u) = u^2. \quad (45)$$

The transfer function of the linearized system at constant input u is given by:

$$H(s,u) = \frac{2\omega_{p_1}^2 u}{s^2 + 2\beta\omega_{p_1}s + \omega_{p_1}^2} \cdot \frac{\omega_{p_2}^2}{s^2 + 2\beta_2\omega_{p_2}s + \omega_{p_2}^2} \cdot \frac{\omega_{p_3}^2}{s^2 + 2\beta_3\omega_{p_3}s + \omega_{p_3}^2}. \quad (46)$$

It is assumed that a low-order parametric model approximation can be obtained at $u = 1.5$ which is accurate up to a frequency $\omega_q = 2$ Hz:

$$H_a(s) = \frac{12\pi^2}{s^2 + 0.8\pi s + 4\pi^2}. \quad (47)$$

To demonstrate robustness of the approach, random variations of the damping and resonance frequencies is applied in the range of 5% of the nominal value to generate a family of ten plants, see the gray lines in Figure 2. The solid black line depicts the low-order approximation H_a.

The dither frequency for classical ESC is selected to be 0.4π with an amplitude of $a = 0.15$. A multisine with $N_k = 4$ is designed with the highest dither frequency $\omega_{N_k} = \omega_q$, see Table 1 for the multisine settings. Fig. 2 shows the dither frequencies with respect to the linearized system dynamics at $u = 1.5$. The amplitude per frequency a is selected such that the peak-to-peak variation of $d(t)$ is the same as in the classical ESC implementation. The optimizer gain is tuned $c = 0.0875$ for both the classical and fast ESC case.

Figure 3 shows the performance of fast ESC in comparison to classical ESC. It can be seen that, the fast ESC

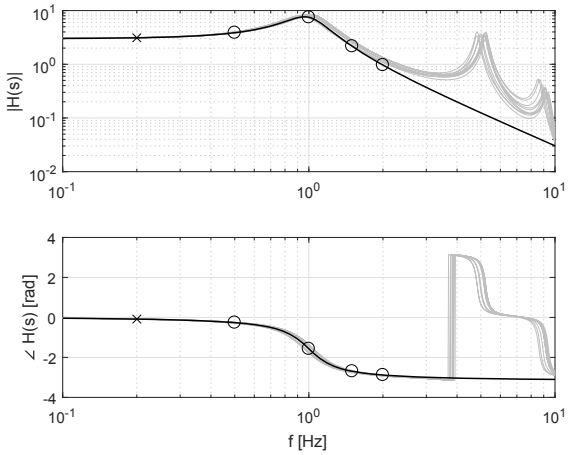

Fig. 2. Bode plot of a family of linearized plant dynamics at $u = 1.5$.

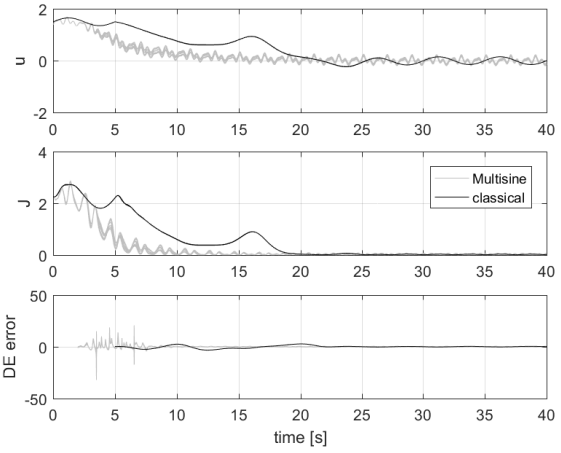

Fig. 3. Trace of extremum seeking control.

converges faster to a neighborhood of the optimum than the classical ESC. The bottom plane shows the DE error calculated with respect to the "true" local gradient of (45). Note that, the classical ESC requires 5s before an accurate DE is available, while the fast ESC only needs 2s. Furthermore, it can be seen that, the performance of fast ESC is robust to the parameter variations.

6. CONCLUSION AND OUTLOOK

The results in this paper enhance the convergence speed of Extremum Seeking Control (ESC) by leveraging from local parametric model techniques. This allows to estimate the gradient of the local steady-state cost using multiple dither frequencies in the range of the system dynamics in conjunction with the aid of frequency-domain analysis and complex curve fitting in a receding horizon fashion. Hence, the time scale separation principle in ESC is relaxed. The transient performance is improved with a factor 4 compared to classical ESC, while robustness to plant uncertainty enables the application of fast ESC. Future work focuses on including measurement noise, delay and multi-input systems.

Table 1. Multisine parameters

k	0	1	2	3
ω_k	0.5	1	1.5	2
a	0.0593	0.0593	0.0593	0.0593
ϕ_k	0.7922	0.9595	0.6557	0.0357

REFERENCES

K.T. Atta and M. Guay. Fast proportional integral phasor extremum seeking control for a class of nonlinear system. *IFAC-PapersOnLine*, 20th IFAC World Congress, Vol. 50, nr. 1, pp. 5724-5730, 2017.

P. Crama, and J. Schoukens. Computing an Initial Estimate of a Wiener-Hammerstein System with a Random Phase Multisine Excitation. *IEEE Transactions on Instrumentation and Measurement*, Vol. 54, No. 1, pp. 117-122, 2005.

M. Haring, N. van de Wouw and D. Nesic. Extremum-seeking control for nonlinear systems with periodic steady-state outputs. *Automatica*, Vol. 49, nr. 6, pp. 1883-1891, 2013.

R. van Herpen, T. Oomen and M. Steinbuch. Optimally Conditioned Instrumental Variable Approach for Frequency-Domain System Identification. *Automatica*, Vol. 50, nr. 9, pp 2281-2293, 2014.

T. van Keulen, L. Huijben and T. Oomen. Identification of control-relevant diesel engine models using a local linear parametric approach. *IFAC-PapersOnLine*, 20th IFAC World Congress, Vol. 50, nr. 1, pp. 7836-7841, 2017.

M. Krstic. Performance improvement and limitations in extremum seeking control. *Systems & Control Letters*, Vol. 39, nr. 5, pp. 313-326, 2000.

M. Krstic and H.H. Wang. Stability of extremum seeking feedback for general nonlinear dynamic systems. *Automatica*, Vol. 36, nr. 4, pp. 595-601, 2001.

E.C. Levy. Complex-Curve fitting. *IRE Transactions on Automatic Control*, Vol. AC-4, pp. 37-44, 1959.

W. Moase and C. Manzie. Fast extremum-seeking for Wiener-Hammerstein plants. *Automatica*, Vol. 48, nr. 10, pp. 2433-2443, 2012.

D. Nesic, Y. Tan, W.H. Moase and C. Manzie. A unifying approach to extremum seeking: Adaptive schemes based on estimation of derivatives. *49th IEEE Conference on Decision and Control (CDC)*, pp. 4625-4630, 2010.

R. Pintelon and J. Schoukens. System identification: a frequency domain approach. *IEEE press*, 2001.

E. Robles, S. Ceballos, J. Pou, J.L. Martin, J. Zaragoza, and P. Ibanez. Variable-Frequency Grid-Sequence Detector Based on a Quasi-Ideal Low-Pass Filter Stage and a Phase-Locked Loop. *IEEE Transactions on Power Electronics*, Vol. 25, nr. 10, pp. 2552-2563, 2010.

C.K. Sanathanan and J. Koerner. Transfer Function Synthesis as a Ratio of Two Complex Polynomials. *Automatica*, Vol. 48, nr. 10, pp. 2433-2443, 1963.

S. Skogestad. Plantwide control: the search for the self-optimizing control structure. *Journal of process control*, Vol. 10, nr. 5, pp. 487-507, 2000.

R. Voorhoeve, T. Oomen, R. van Herpen and M. Steinbuch. On numerically reliable frequency-domain system identification: new connections and a comparison of methods. *IFAC-PapersOnLine*, 19th IFAC World Congress, pp. 10018-10023, 2014.

A.H. Whitfield. Asymptotic behaviour of transfer function synthesis methods. *International Journal of Control*, Vol. 45, pp. 1083-1092, 1987.